H_0 tension, phantom dark energy, and cosmological parameter degeneracies

G. Alestas,* L. Kazantzidis,† and L. Perivolaropoulos‡
Department of Physics, University of Ioannina, GR-45110 Ioannina, Greece

(Received 28 April 2020; accepted 2 June 2020; published 16 June 2020)

Phantom dark energy ($w < -1$) can produce amplified cosmic acceleration at late times, thus increasing the value of H_0 favored by CMB data and releasing the tension with local measurements of H_0. We show that the best fit value of H_0 in the context of the CMB power spectrum is degenerate with a constant equation-of-state parameter w, in accordance with the approximate effective linear equation $H_0 + 30.93w - 36.47 = 0$ (H_0 in $\mathrm{km\,sec^{-1}\,Mpc^{-1}}$). This equation is derived by assuming that both $\Omega_{0m}h^2$ and $d_A = \int_0^{z_{\rm rec}} \frac{dz}{H(z)}$ remain constant (for an invariant CMB spectrum) and equal to their best fit *Planck*/ΛCDM values as H_0, Ω_{0m}, and w vary. For $w = -1$, this linear degeneracy equation leads to the best fit $H_0 = 67.4\ \mathrm{km\,sec^{-1}\,Mpc^{-1}}$ as expected. For $w = -1.22$, the corresponding predicted CMB best fit Hubble constant is $H_0 = 74\ \mathrm{km\,sec^{-1}\,Mpc^{-1}}$, which is identical with the value obtained by local-distance ladder measurements, while the best fit matter density parameter is predicted to decrease, since $\Omega_{0m}h^2$ is fixed. We verify the above $H_0 - w$ degeneracy equation by fitting a wCDM model with fixed values of w to the *Planck* TT spectrum, showing also that the quality of fit (χ^2) is similar to that of ΛCDM. However, when including SnIa, baryon acoustic oscillation, or growth data, the quality of fit becomes worse than ΛCDM when $w < -1$. Finally, we generalize the $H_0 - w(z)$ degeneracy equation for the parametrization $w(z) = w_0 + w_1 z/(1+z)$ and identify analytically the full $w_0 - w_1$ parameter region (straight line) that leads to a best fit $H_0 = 74\ \mathrm{km\,sec^{-1}\,Mpc^{-1}}$ in the context of the *Planck* CMB spectrum. This exploitation of $H_0 - w(z)$ degeneracy can lead to immediate identification of all parameter values of a given $w(z)$ parametrization that can potentially resolve the H_0 tension.

DOI: 10.1103/PhysRevD.101.123516

I. INTRODUCTION

The discrepancy in the value of the Hubble parameter as obtained from the cosmic microwave background (CMB) and baryon acoustic oscillation (BAO) data ($67.4 \pm 0.5\ \mathrm{km\,sec^{-1}\,Mpc^{-1}}$) [1,2] and local-distance ladder measurements ($H_0 = 74.03 \pm 1.42\ \mathrm{km\,sec^{-1}\,Mpc^{-1}}$) [3] has reached a level close to 6σ [4–8] and is becoming a problem of the standard ΛCDM model. A similar issue, with a lower significance level, appears when measuring the growth rate of cosmological perturbations using peculiar velocities (redshift space distortions) [9–14] and weak lensing [15–19] cosmological data. Such measurements find a weaker growth rate of perturbations than anticipated in the context of the standard ΛCDM model [9,13,14,17,18,20]. This weaker growth is expressed in the context of ΛCDM parameters as a lower best fit value of the matter density parameter $\Omega_{0m} \approx 0.28 \pm 0.03$ [18,21] than the one anticipated in the context of geometric probes including the CMB spectrum peak locations [1,2] and the BAO data [22–24] in the context of a flat ΛCDM model ($\Omega_{0m} = 0.315 \pm 0.007$).

Other independent groups studying local expansion [25–30] find a lower value of H_0 compared to Ref. [3] with larger error bars, reducing the effect of the tension to approximately 2σ. Moreover, independent measurements of the Hubble constant using $H(z)$ measurements [31–35], γ rays [36,37], BAO measurements [38], as well as various combinations of data [39–45] report a value for H_0 that is lower than the one provided by the local measurements and in consistency with the CMB measurement.

A wide range of models have been used to explain these tensions and properly extend ΛCDM using specific new degrees of freedom (for a quantitative measure of tensions, see Refs. [46–48]). For the Hubble tension, these models include mechanisms that modify the scale of the sound horizon at last scattering using early dark energy [49–54] or other types of early species [55–57], interacting dark energy with matter [58–63], screened fifth forces on the cosmic distance ladder [64,65], modified gravity [66–70], local matter underdensities [71], and new properties of late dark energy including new types of dark energy equation-of-state parameters [72–74]. For the growth tension, modified gravity [13,14,75–78], running vacuum models [79,80], nonzero spatial curvature [81,82], and modification of dark energy properties [80,83–90] have also been considered.

*g.alestas@uoi.gr
†l.kazantzidis@uoi.gr
‡leandros@uoi.gr

In both types of tension, it has become clear that new properties of dark energy may constitute the required missing degree of freedom. In particular, it has been shown that a mildly phantom dark energy with an equation of state parameter evolving slightly below $w = -1$ has the potential to resolve the Hubble tension by amplifying late-time acceleration, which leads to an increased best value of the Hubble parameter H_0 in the context of the CMB data, thus bringing it close to the value obtained by local-distance ladder measurements [72,74,74,91–95]. Most previous analyses along the above lines utilize evolving equation-of-state parameters that in many cases have sophisticated functional forms. Even though such functional forms of $w(z)$ usually involve at most one new parameter, these approaches have two drawbacks: complexity of the $w(z)$ considered forms and a worse fit than ΛCDM to the *Planck* CMB TT power spectrum and other cosmological data ($\Delta\chi^2 > 0$). Thus, these models are usually not favored [96] compared to ΛCDM in the context of information criteria that penalize models with additional parameters if they do not improve the quality of fit to data. It would therefore be desirable to construct models/parametrizations with no new parameters that can potentially resolve both the Hubble and growth tensions by modifying the dark energy properties.

In particular, the following questions need to be addressed:

(1) What are the properties of the new phantom degree of freedom required in order to increase the best fit value of H_0 in the context of CMB data to the level required for consistency with local measurements and resolution of the H_0 tension?
(2) What are the corresponding best fit values of cosmological parameters that emerge in the context of this type of phantom dark energy, and to what extent do they lead to improvement of the resolution of the growth tension?
(3) What is the quality of fit of these extended models to the CMB *Planck* and other cosmological data, and how does it compare with the corresponding quality of fit of ΛCDM?

The goal of the present analysis is to address these questions using an approximate analytical method utilizing the degeneracies of cosmological parameters with respect to the form of the CMB power spectrum. In addition, we utilize more accurate numerical estimates of best fit cosmological parameters using Boltzmann and Markov chain–Monte Carlo (MCMC) codes. In the context of the analytical approximation, we exploit the degeneracies of the CMB power spectrum among different cosmological parameter combinations and explore the consequences of variations of the dark energy equation-of-state parameter $w(z)$ on other cosmological parameters, and in particular on the Hubble parameter H_0 and the matter density parameter Ω_{0m}.

The structure of this paper is the following: In Sec. II, we review the well-known degeneracies of the CMB TT power spectrum and identify the five cosmological parameter combinations that to a great extent uniquely determine the form of the spectrum. By demanding that these five combinations remain fixed to their *Planck*/ΛCDM values, we identify the expected change of the best fit values of specific parameters including the Hubble parameter H_0 and the matter density parameter Ω_{0m} when the form of the dark energy equation-of-state parameter $w(z)$ changes. Thus, we identify the forms of $w(z)$ leading to a value of H_0 consistent with local-distance ladder measurements. In Sec. III, we fix $w(z)$ to the forms predicted analytically for the resolution of the H_0 tension and identify numerically the best fit cosmological parameters using Boltzmann and MCMC codes with *Planck* CMB data. We also compare the numerically obtained best fit cosmological parameter values with the corresponding values obtained in the context of the analytical approximation of Sec. II for the same form of $w(z)$. Finally, in Sec. IV, we summarize and discuss possible extensions of this analysis.

II. CMB SPECTRUM DEGENERACIES AND THE $H_0(w)$ DEPENDENCE

It is well known [97,98] that the form of the CMB temperature power spectrum is almost uniquely determined if the following parameter combinations are fixed:

(1) The matter density parameter combination $\omega_m \equiv \Omega_{0m}h^2$, where $H_0 = 100\ \mathrm{km\,sec^{-1}\,Mpc^{-1}}$.
(2) The baryon density parameter combination $\omega_b \equiv \Omega_{0b}h^2$, where Ω_{0b} is the present-day baryon density parameter.
(3) The radiation density parameter combination $\omega_r \equiv \Omega_{0r}h^2$, where Ω_{0r} is the present-day radiation density parameter.
(4) The primordial fluctuation spectrum.
(5) The curvature parameter $\omega_k = \Omega_{0k}h^2$.
(6) The flat-universe comoving angular diameter distance to the recombination surface,

$$d_A(\omega_m, \omega_r, \omega_b, h, w(z)) = \int_0^{z_r} \frac{dz}{H(z)}, \tag{2.1}$$

where $z_r \simeq 1100$ is the redshift of recombination provided to better accuracy as [99]

$$\begin{aligned} z_r &= 1048(1 + 0.00124\omega_b^{-0.738})(1 + g_1\omega_m^{g_2}), \\ g_1 &= 0.0783\omega_b^{-0.238}/(1 + 39.5\omega_b^{0.763}), \\ g_2 &= 0.560/(1 + 21.1\omega_b^{1.81}), \end{aligned} \tag{2.2}$$

and $H(z)$ is the Hubble parameter at redshift z. The Hubble parameter takes the form

$$H(z,\omega_m,\omega_r,\omega_b,h,w(z)) = H_0\sqrt{\Omega_{0m}(1+z)^3+\Omega_{0r}(1+z)^4+\Omega_{0\mathrm{de}}e^{3\int_0^z dz'(1+w(z'))/(1+z')}}, \tag{2.3}$$

where $w(z)$ is the dark energy equation-of-state parameter at redshift z and $\Omega_{0\mathrm{de}} = 1-\Omega_{0m}-\Omega_{0r}$ is the present-day value of the dark energy density parameter. The product $\sqrt{\omega_m}\cdot d_A$ is independent of H_0 and constitutes the well-known shift parameter defined as [97,100]

$$R = \sqrt{\omega_m}\int_0^{z_r}\frac{dz}{H(z)}. \tag{2.4}$$

The observed values of the above parameter combinations as determined by the *Planck*/ΛCDM CMB temperature power spectrum are the following [2]:

$$\bar{\omega}_m = 0.1430\pm 0.0011, \tag{2.5}$$

$$\bar{\omega}_b = 0.02237\pm 0.00015, \tag{2.6}$$

$$\bar{\omega}_r = (4.64\pm 0.3)10^{-5}, \tag{2.7}$$

$$\bar{\omega}_k = -0.0047\pm 0.0029, \tag{2.8}$$

$$\bar{d}_A = (100\ \mathrm{km\,sec^{-1}\,Mpc^{-1}})^{-1}(4.62\pm 0.08), \tag{2.9}$$

where for the radiation density we have assumed three relativistic neutrino species.

These parameter combinations also express the approximate degeneracy of the CMB with respect to various specific cosmological parameters. For example, if the first four parameter combinations are fixed [Eqs. (2.5)–(2.8)], the fifth constraint [Eq. (2.9)] provides the analytically predicted best fit value of the Hubble parameter H_0 (or h) given the dark energy equation-of-state parameter $w(w_0,w_1,\ldots,z)$, where $w_0,w_1,\ldots$ are the parameters entering the $w(z)$ parametrization.[1] Thus, it is straightforward to use Eqs. (2.1), (2.3), (2.5), and (2.9) to construct the function $h(w_0,w_1,\ldots)$ that gives semianalytically the predicted best fit value of h given a specific form of $w(z)$. This function is derived by solving the following equation with respect to h:

$$d_A(\bar{\omega}_m,\bar{\omega}_r,\bar{\omega}_b,h=0.674,w=-1) = d_A(\bar{\omega}_m,\bar{\omega}_r,\bar{\omega}_b,h,w(z)). \tag{2.10}$$

In the context of a simple one-parameter parametrization where $w(z)$ remains constant in time and redshift (wCDM model), Eq. (2.3) takes the simple form

$$H(z,\omega_m,\omega_r,\omega_b,h,w(z)) = H_0\sqrt{\Omega_{0m}(1+z)^3+\Omega_{0r}(1+z)^4+(1-\Omega_{0m}-\Omega_{0r})(1+z)^{3(1+w)}}, \tag{2.11}$$

and using the above described approach, by solving Eq. (2.10), it is straightforward to derive the degeneracy function $h(w)$ shown in Fig. 1 (continuous orange line). In the range $w\in[-1.5,-1]$, $h(w)$ is approximated as a straight line (dashed blue line in Fig. 1):

$$h(w)\approx -0.3093w+0.3647. \tag{2.12}$$

The points with the error bars were obtained by fitting to the *Planck*/CMB power spectrum using the corresponding wCDM models with fixed w. This analysis is discussed in more detail in the next section. In Fig. 2, we show the predicted form of the CMB TT anisotropy spectrum for $w=-1$ ($h=0.67$, $\Omega_{0m}=0.314$) and $w=-1.2$ ($h=0.74$, $\Omega_{0m}=0.263$), demonstrating the invariance of the CMB power spectrum when the cosmological parameters are varied along the above described degeneracy directions.

The dark energy equation-of-state parameter value leading to $h(w)=0.74$ is $w\approx -1.217$, which is the predicted value of w required to alleviate the H_0 tension, a result consistent with previous studies [91,92]. In particular, a related analysis has been performed in Ref. [91], where the author points out that fixing the dark energy equation of state $w\approx -1.3$ or the effective number of relativistic species $N_{\mathrm{eff}}\approx 3.95$ may lead to the relaxation of the H_0 tension. The novel feature of our work is the use of analytical methods to identify the qualitative features required for any form of $w(z)$ to relax the H_0 tension.

This method for deriving the predicted dark energy properties required to resolve the H_0 tension may be

[1] In the present analysis, we assume a flat universe and fix $\bar{\omega}_k = 0$.

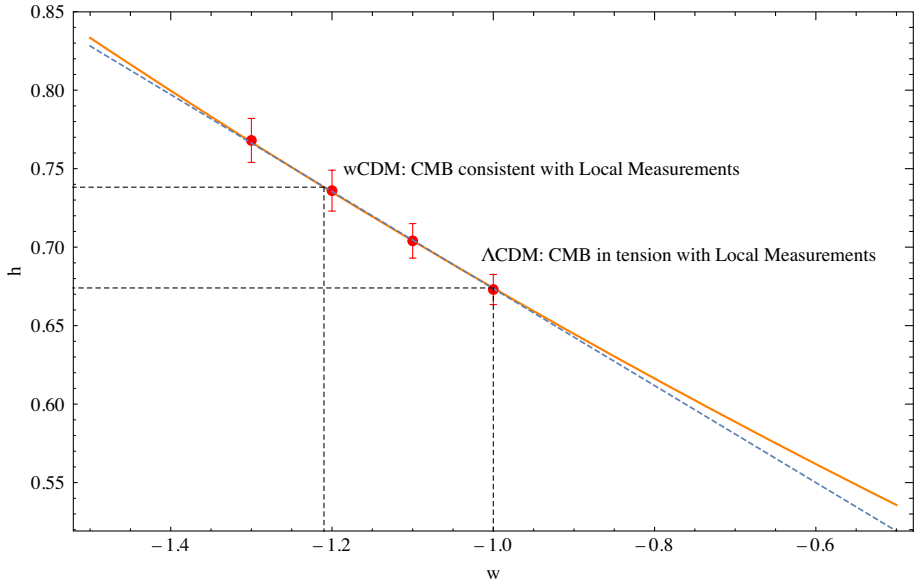

FIG. 1. The predicted value of h as a function of the fixed w for the one-parameter dark energy (wCDM) model. The orange line corresponds to the theoretically predicted best fit values of h for different values of w in the case of the wCDM model, whereas the dashed blue line corresponds to the linear fitting that has been made. The red points display the actual best fit values, including the error bars, of h for specific values of w obtained by fitting these models to the CMB TT anisotropy via the MGCosmoMC (see Table II).

extended to more parametrizations of $w(z)$. For example, in the case of the two-parameter CPL parametrization [101,102] expansion of $w(z)$,

$$w = w_0 + w_1(1-a) = w_0 + w_1 z/(1+z), \tag{2.13}$$

Eq. (2.3) is written as

$$H(z) = H_0\sqrt{\Omega_{0m}(1+z)^3 + \Omega_{0r}(1+z)^4 + (1-\Omega_{0m}-\Omega_{0r})(1+z)^{3(1+w_0+w_1)}e^{-3\frac{w_1 z}{1+z}}}. \tag{2.14}$$

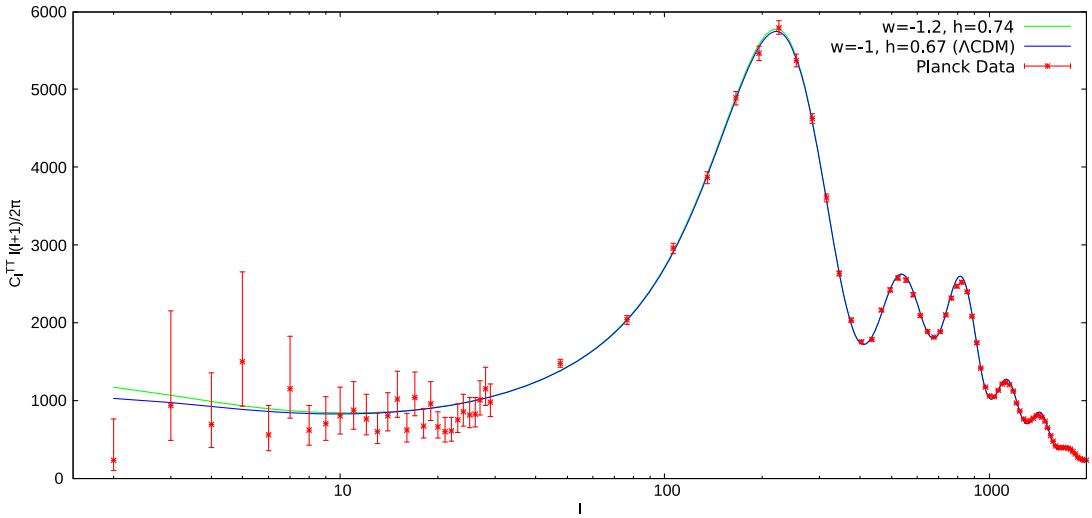

FIG. 2. The CMB power spectrum for ΛCDM (blue line) and $w = -1.2$ (green line). We also show the binned high-l and low-l *Planck* data (red points).

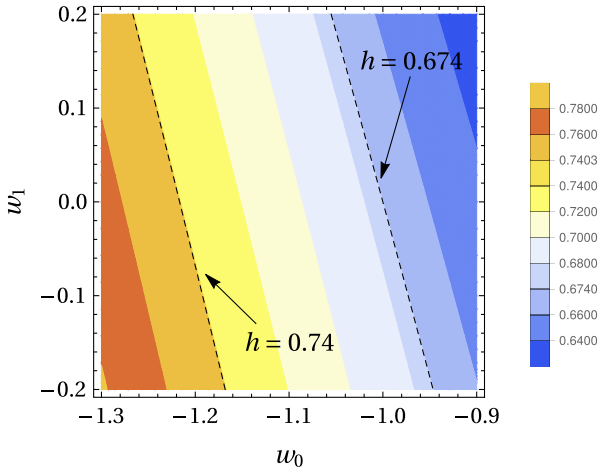

FIG. 3. The degeneracy with respect to the CMB spectrum in the parameter space $(w_0 - w_1)$. The dashed lines correspond to $h = 0.674$ (ΛCDM value) and to $h = 0.74$ (the value of Ref. [3]).

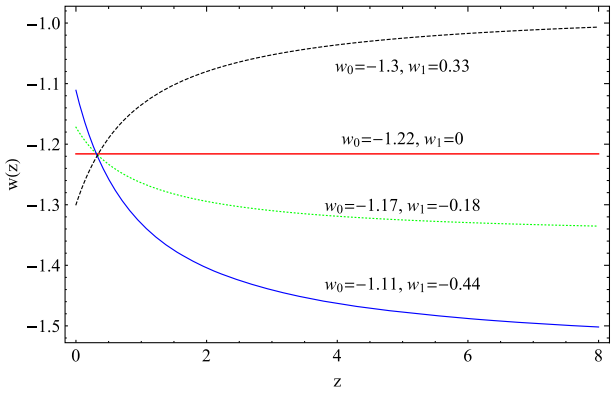

FIG. 4. The evolution of $w(z)$ for various values of (w_0, w_1) along the degeneracy $h = 0.74$ line of Fig. 3. All these parameter values lead to a best fit value $h = 0.74$ in the context of the CMB power spectrum. However, they do not have the same quality of fit to other cosmological data which can be used to break this model degeneracy. The common (z, w) point of intersection of all the $w(z)$ plots is $(0.31, -1.22)$.

Using now Eqs. (2.1), (2.5), (2.9), and (2.12) in the context of the above described method, it is straightforward to derive the degeneracy function $h(w_0, w_1)$, by solving Eq. (2.10). This is shown in Fig. 3. The dashed lines correspond to the parameter values that satisfy $h(w_0, w_1) = 0.674$ [the ΛCDM value, which as expected goes through the point $(w_0, w_1) = (-1, 0)$] and $h(w_0, w_1) = 0.74$ [the local-distance ladder measurements value]. The constant h lines shown in Fig. 3 are approximately straight lines in the range of the $w_0 - w_1$ parameter space shown in Fig. 3. In particular, for the case of the value $h = 0.74$, which alleviates the H_0 tension, this line is approximated by the equation

$$w_1 \approx -4.17 w_0 - 5.08. \tag{2.15}$$

Clearly, the preference for a phantom-like behavior $w(z) < -1$ in the context of the local measurement value of h, at least for some redshift range, is apparent in Fig. 3. This is also demonstrated in Fig. 4, where we show four forms of $w(z)$ based on the CPL parametrization that can resolve the H_0 tension by providing a best fit value of $h = 0.74$ from the CMB data. The corresponding wCDM value of $w = -1.22$ is also shown. Clearly, all degenerate forms of CPL $w(z)$ that relax the H_0 tension go through the same point at $z = 0.31$, crossing the $w = -1.22$ line. This type of degeneracy in particular redshifts for cosmological parameters has been discussed in Ref. [103]. Also, degenerate $w(z)$ curves with $w_0 < 1.22$ are increasing functions of z, while those with $w_0 > 1.22$ are decreasing functions of z. This appears to be a general feature of all $w(z)$ parametrizations that can relax the H_0 tension. For example, the PEDE parametrization [74] and the late dark energy transition hypothesis [104] with $w(z \simeq 0) > -1.22$ are decreasing functions of the redshift z as predicted by the above degeneracy analysis. The identification of these properties opens up the possibility of a very late phase-type transition at $z \simeq 0.01$ from a phantom phase to a ΛCDM phase with a sharply increasing rather than decreasing function of $w(z)$.

Even though the approximate parameter degeneracy exploited in this section is useful for the derivation of the forms of $w(z)$ that can alleviate the H_0 tension, an important fact that needs to be considered is the quality of fit of the preferred degenerate forms of $w(z)$ to other cosmological data like SnIa, BAO, and growth of perturbations data [redshift space distortion $f\sigma_8(z)$ and weak lensing data], as well as to actual CMB power spectrum data which may not fully respect the above exploited approximate degeneracy (especially at low l). Such a fit to cosmological data beyond the CMB is expected to break the above degeneracy obtained from the CMB spectrum. Even if particular forms of $w(z)$ can lead to apparent alleviation of the H_0 tension, such a solution would not be preferable if the quality of fit to the actual CMB spectrum and to other cosmological data is significantly degraded compared to ΛCDM ($w = -1$). Thus, in the next section, we address the following questions:

(1) What is the quality of fit of the forms of $w(z)$ that are predicted to resolve the H_0 tension, on cosmological data involving SnIa, BAO, growth redshift space distortion data, and the actual *Planck* CMB TT power spectrum data? Is this quality of fit (χ^2) similar to the corresponding quality for ΛCDM?
(2) Is the H_0 tension actually alleviated when the full CMB spectrum data are used in the context of a model with fixed $w(z)$ to its predicted form (e.g., $w = -1.22$ in the context of a constant w)?
(3) Is the growth tension partially relaxed in the context of the above preferred $w(z)$ found?

These questions will be addressed mainly in the context of a redshift-independent w, but it is straightforward to generalize the analysis for more general forms of $w(z)$.

III. NUMERICAL ANALYSIS OF DARK ENERGY MODELS

In order to test the resolution of the H_0 tension and test the quality of fit to the CMB and other cosmological data of the models discussed in the previous section, we use the MGCosmoMC numerical package [105–107] with the *Planck* dataset. In particular, we use the *Planck* TT and lowP dataset, i.e., the TT likelihood for high-l multipoles ($l > 30$) as well as the *Planck* temperature and polarization data for low multipoles ($l < 30$). The priors that have been used as input can be seen in Table I.

We fix w to the values of the points shown in Fig. 1 ($w = -1.0, -1.1, -1.2, -1.3$) and construct the likelihood contours for the cosmological parameters of these four models. The resulting best fit values of h are shown in Table II (see also Fig. 1) and are in excellent agreement with the expectations based on the parameter degeneracy analysis of the previous section (orange continuous line in Fig. 1). The corresponding likelihood contours are shown in Fig. 5.

Clearly, the likelihood contours for the Hubble parameter shift to higher best fit values as w decreases in the phantom regime ($w < -1$). At the same time, the best fit values of the matter density parameter Ω_{0m} decrease in accordance with the degenerate parameter combination $\Omega_{0m}h^2$.

This reduced value of the best fit Ω_{0m} would naively imply reduced growth of cosmological perturbations and thus resolution of the growth tension. However, the reduced best fit value of the matter density parameter Ω_{0m} is not enough to soften the growth tension, since the best fit value of the parameter σ_8 (the present-day rms matter fluctuations variance on scales of $8h^{-1}$ Mpc) appears to increase more rapidly, as w decreases in the phantom regime. Since this parameter is proportional to the initial amplitude of the matter perturbation power spectrum, its increase amplifies the growth of perturbations and tends to cancel the effect of the decrease of the best fit Ω_{0m} in the context of perturbation growth. This is demonstrated in Fig. 6, where we show the σ_8 likelihood contours obtained by fitting the models $w = -1$ (ΛCDM) and $w = -1.2$ to the growth $f\sigma_8$ data (we have used the conservative robust dataset of Table 2 of Ref. [108], a subset of an up-to-date compilation presented in Ref. [109]). Superimposed, we also show the corresponding likelihood contours obtained from the *Planck* CMB TT power spectrum obtained for each value of fixed w. Clearly, the tension between the RSD $f\sigma_8$ data and the *Planck* data increases in the context of the phantom model $w = -1.2$ compared to ΛCDM ($w = -1$).

In addition to the growth data, we also fit the models $w = -1$ and $w = -1.2$ to a cosmological data combination including the Pantheon SnIa [110], BAO data [23,111,112], and CMB data [1], as well as the prior of the Hubble constant published by Riess *et al.* [3], and obtain for ΛCDM $\chi^2 = 12319.2$, while for $w = -1.2$ we obtain $\chi^2 = 12332.7$. We thus find $\Delta\chi^2 = 13.5$. This difference of $\Delta\chi^2 = 13.5$ for the phantom model indicates a significantly reduced quality of fit compared to ΛCDM in agreement with previous studies [113]. The corresponding likelihood contours are shown in Fig. 7. It is therefore clear that the particular fixed-w models considered here lead to an apparent resolution of the Hubble tension, since they increase the best fit value of H_0 in the context of the CMB data, but the resolution is not viable, since the growth tension gets worse while the quality of fit of these models to the SnIa and BAO data is not as good as for ΛCDM. This result is consistent with previous studies [92], where it has been demonstrated that non-CMB data such as BAO and SNIa favor lower values of H_0 which are more consistent with the CMB value, while also disfavoring $w < -1$ in the context of flat and nonflat untilted inflation models [42]. It is, however, worth mentioning that for the combination of the CMB *Planck* data and the Riess Hubble constant prior,

TABLE I. The MGCosmoMC priors that have been used in Figs. 5 and 7. We also set $A_{\rm lens} = 1$ and $\Omega_k = 0$.

Parameters	Priors
$\Omega_b h^2$	[0.005, 0.1]
$\Omega_c h^2$	[0.001, 0.99]
$100\theta_{\rm MC}$	[0.5, 10]
τ	[0.06, 0.8]
$\ln(10^{10}A_s)$	[1.61, 3.91]
n_s	[0.8, 1.2]

TABLE II. The analytically predicted CMB best fit values of h and Ω_{0m} for fixed w, obtained by using the CMB parameter degeneracy arguments, as well as the ones obtained by the actual fit of the corresponding w model to the *Planck* TT CMB anisotropy power spectrum. The quality of fit for each model compared to ΛCDM is also indicated by the value of $\Delta\chi^2$.

w	$\Omega_{0m}^{\rm th}$	$h_{\rm th}$	$\Omega_{0m}^{\rm obs}$	$h_{\rm obs}$	$\chi^2_{\rm CMB}$	$\Delta\chi^2_{\rm CMB}$
-1.0	0.316	0.674	0.315 ± 0.013	0.673 ± 0.010	11266.516	$\cdots$
-1.1	0.289	0.704	0.288 ± 0.013	0.704 ± 0.011	11266.530	0.014
-1.2	0.265	0.735	$0.263^{+0.012}_{-0.014}$	0.736 ± 0.013	11267.132	0.616
-1.3	0.244	0.766	$0.242^{+0.012}_{-0.013}$	0.768 ± 0.014	11266.520	0.004

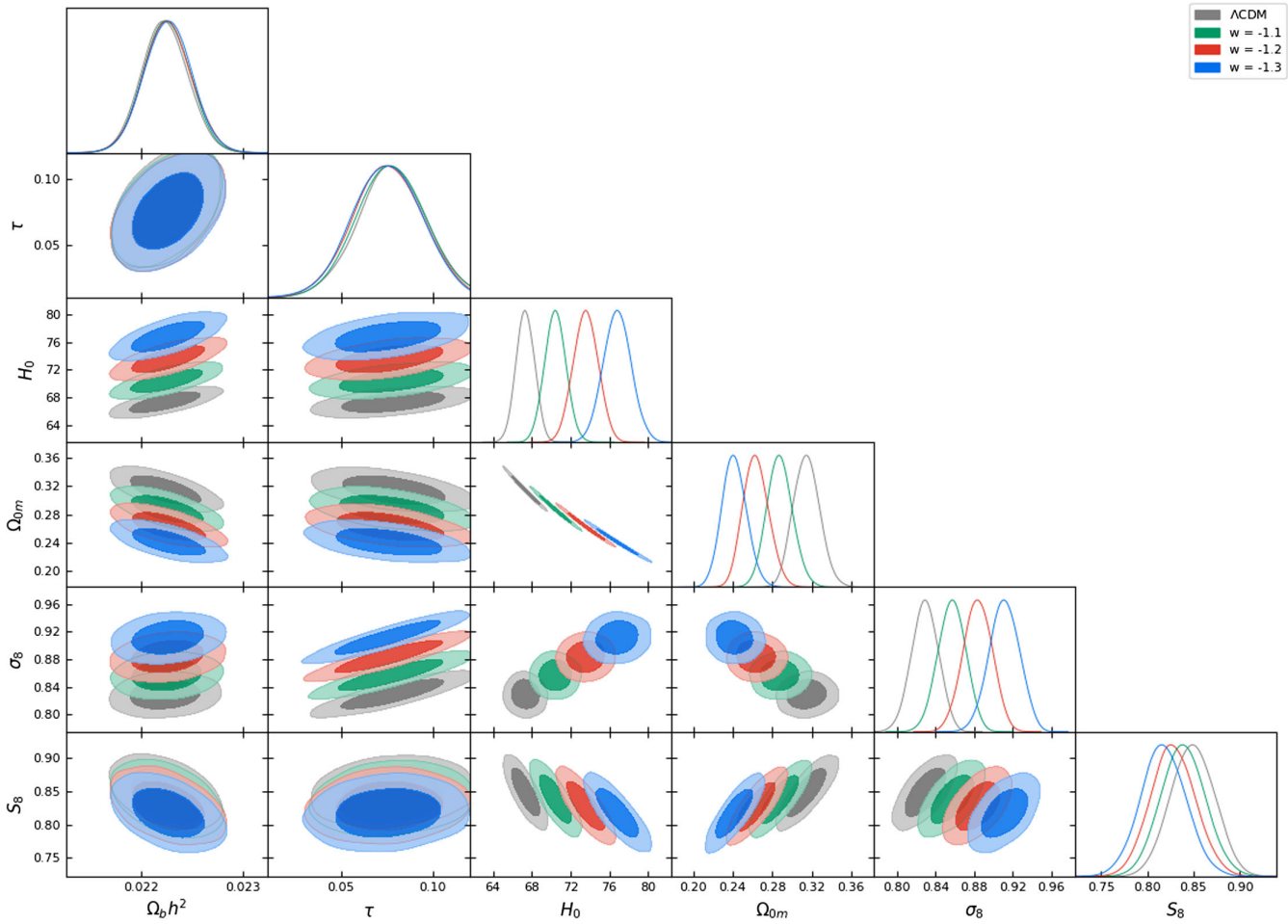

FIG. 5. The contour plots constructed with MGCosmoMC using the *Planck* TT and lowP likelihoods for ΛCDM and *w*CDM models. The gray contours correspond to the ΛCDM model. The green contours correspond to $w = -1.1$, the red ones to $w = -1.2$, and the blue to $w = -1.3$. For $w = -1.1$, the best fit value of H_0 is close to that of the *Planck*/ΛCDM measurement [1], while the $w = -1.2$ and $w = -1.3$ values shift h closer to the local-distance ladder measurements [3].

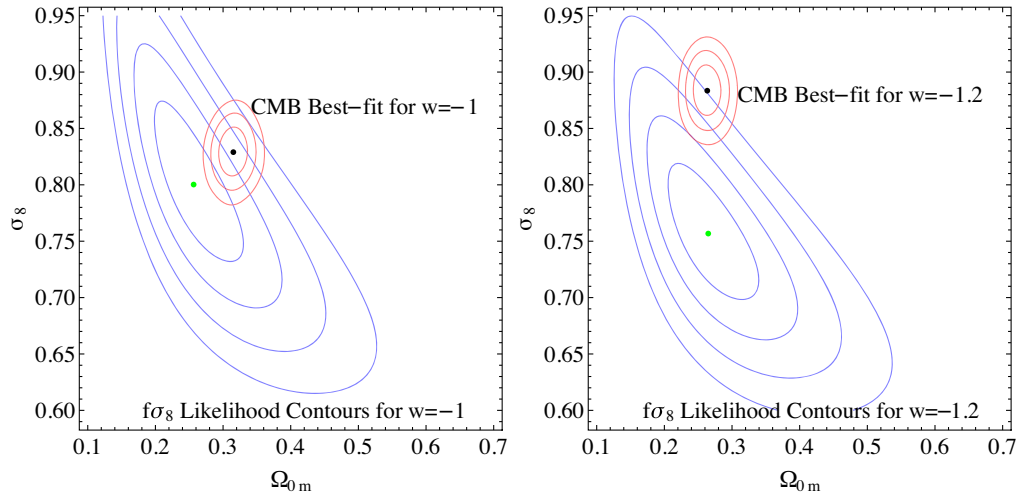

FIG. 6. The 1σ–4σ contours in the parametric space $\Omega_{0m} - \sigma_8$. The blue contours correspond to the best fit growth compilation of Ref. [108], while the red contours correspond to the 1σ–4σ confidence contours for $w = -1$ (left panel) and $w = -1.2$ (right panel) obtained from the *Planck* data.

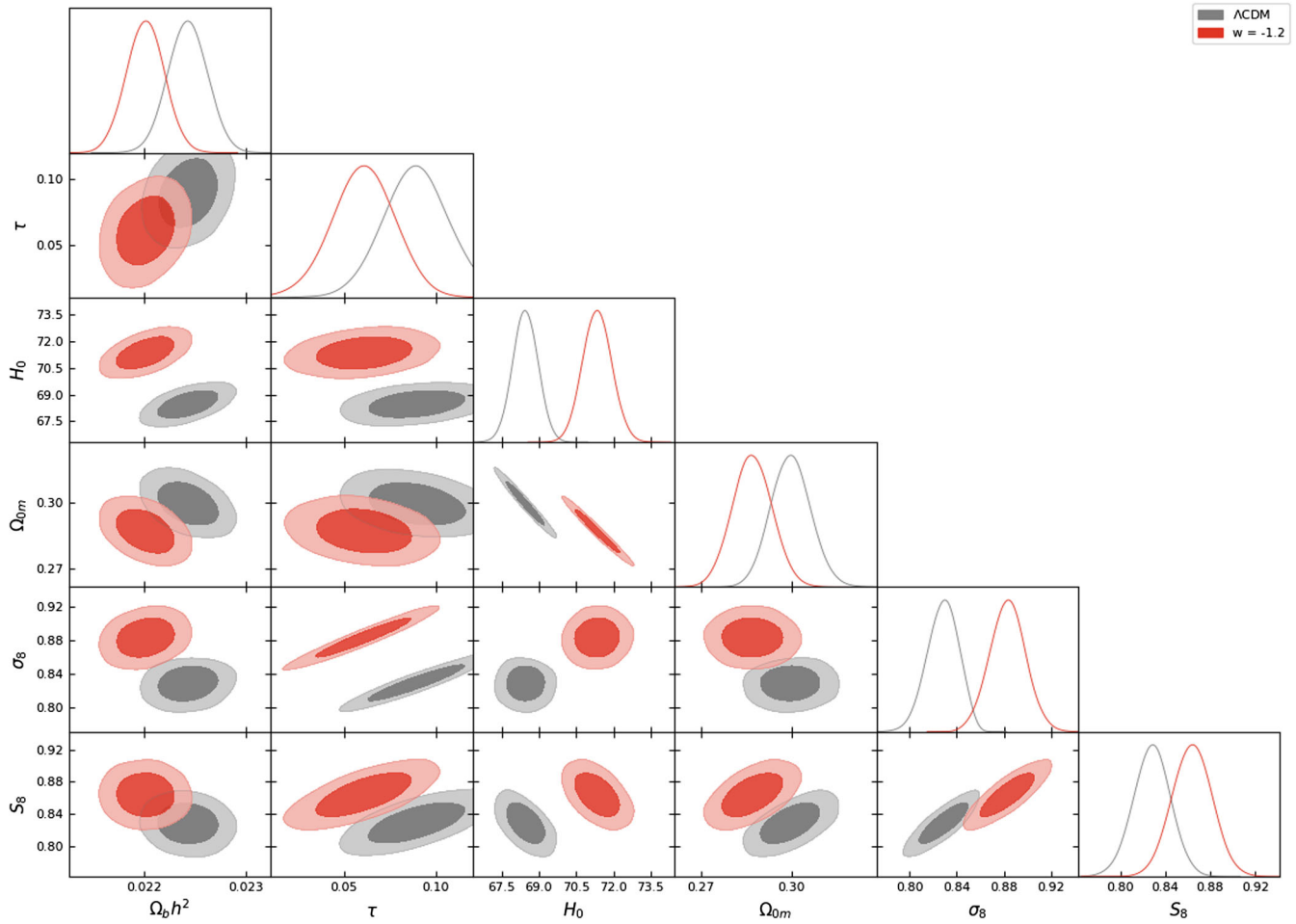

FIG. 7. The likelihood contours constructed with MGCosmoMC using the cosmological data combination of Pantheon SnIa [110], BAO data [23,111,112], and CMB data [1], as well as the prior of the Hubble constant [3] for ΛCDM (gray contours) and wCDM with $w = -1.2$ (red contours).

the quality of the fit improves drastically for $w = -1.2$, with $\Delta\chi^2 = -10.7$ in respect to $w = -1$. The exploitation of the CMB spectrum degeneracy of more complicated forms of $w(z)$, however, may lead to better fits to growth, SnIa, and BAO cosmological data.

IV. CONCLUSION—DISCUSSION—OUTLOOK

We have used analytical degeneracy relations among cosmological parameters and numerical fits to cosmological data to identify the qualitative and quantitative features of dark energy models that have the potential to relax the H_0 tension of the ΛCDM model. We have found that mildly phantom models with mean equation-of-state parameter $w \simeq -1.2$ have the potential to alleviate this tension. The models may be constructed in such a way that there are no extra parameters compared to ΛCDM by using fixed parametrizations of $w(z)$. In practice, however, these models involve more fine-tuning compared to ΛCDM and are clearly less natural than the standard model. In addition, the quality of fit of the simplest of such models to cosmological data beyond the CMB is not as good as the corresponding quality of fit of ΛCDM. However, it is straightforward to construct physical models involving either a phantom scalar field with noncanonical kinetic terms or modified gravity models that naturally produce the required phantom behavior of dark energy. Despite the usual stability issues of such models, it is possible to construct ghost-free versions [114]. For example, physical models described by scalar field Lagrangians can reproduce an effective dark energy with a constant equation-of-state parameter w in the context of both quintessence ($w > -1$) [115–117] and phantom dark energy ($w < -1$) [118].

In particular, a dynamical dark energy scalar field with an inverse power-law potential of the form $V(\phi) = M^{(4+\alpha)}\phi^{-\alpha}$ (where M and $\alpha > 0$ are free parameters) corresponds to a physically interesting model where the dark energy equation-of-state parameter w is constant and takes the form [117]

$$w = \frac{\frac{\alpha}{2} w_B - 1}{1 + \frac{\alpha}{2}} \tag{4.1}$$

where w_B is the equation-of-state parameter of the dominant background. Clearly, for a matter-dominated epoch ($w_B = 0$), and $\alpha > 0$, we can obtain a constant w and a quintessence-like behavior ($w > -1$).

Similarly, a phantom-like behavior ($w < -1$) with constant w may be obtained [118] in the context of a scalar field with noncanonical kinetic terms with an action of the form

$$S = \int d^4x\sqrt{-g}\left(\frac{1}{2\kappa^2}R + p(\phi, \nabla\phi)\right) + S_B, \tag{4.2}$$

where $\kappa^2 = 8\pi G$ and S_B is the action of the background. The Lagrangian may be assumed to depend only on the scalar field ϕ and its derivative squared, $X = -\frac{1}{2}\nabla^\mu\phi\nabla_\mu\phi$. In the case of a slowly varying field X, the pressure p and energy density ρ of the field take the form [118]

$$p = f(\phi)(-X + X^2), \tag{4.3}$$

$$\rho = 2X\frac{\partial p}{\partial X} - p = f(\phi)(-X + 3X^2). \tag{4.4}$$

For $f(\phi) \propto \phi^{-\alpha}$, Eqs. (4.3) and (4.4) lead to an equation-of-state parameter of the form

$$w = \frac{(1 + w_B)\alpha}{2} - 1. \tag{4.5}$$

For a matter-dominated epoch ($w_B = 0$), an appropriate value of α can lead to either a quintessence or a phantom behavior. In particular, for $\alpha < 2$ we obtain $w > -1$ (quintessence behavior), while for $a < 0$ we obtain a physical model with $w < -1$ (phantom equation of state).

However, the constant-w behavior of both of the above physical models described by Eqs. (4.1) and (4.5) is a good approximation only in the context of a dominant background fluid with constant equation of state w_B. In our Universe, this would occur, for example, only well in the matter-dominated epoch. These equation-of-state parameters would cease to have a constant form near the end of the matter era and in the present transition cosmological era. Thus, the constancy of w in the context of these physical models is a good approximation only on high redshifts ($z > 2$).

Interesting extensions of the present analysis include the following:

(1) A comparative analysis of phantom models identified using the degeneracy analytical method proposed here, involving also the redshift dependence of $w(z)$. Such an analysis would rank these models according to their quality of fit on cosmological data.
(2) The construction of physical models that can reproduce the forms of $w(z)$ required to relax the H_0 and possibly the growth tension as well, while providing a better fit to the cosmological data than the fit of ΛCDM. The construction of stable theories with phantom behavior is possible in the context of modified gravity theories. In many such theories, however, including $f(R)$ and scalar-tensor theories, it is not possible to combine stability with the weaker gravity and phantom behavior [119,120] required for the resolution of the H_0 and growth tensions.

The analytical approach for the $H_0 - w(z)$ degeneracy pointed out in the present analysis offers a new method to systematically search and design $w(z)$ forms that can combine the proper features required to consistently relax the tension while keeping a good fit to other cosmological data. Our goal here was only to introduce the method and apply it to the simplest cases while also pointing out the difficulties in resolving the tension. In a subsequent full application and extension of the method, we plan to exploit its full potential in identifying possible forms of $w(z)$ that can actually resolve the tension while keeping a good fit to other cosmological data.

Numerical Analysis Files: The numerical files for the reproduction of the figures can be found in Ref. [121].

ACKNOWLEDGMENTS

We thank Savvas Nesseris for his help with the MGCosmoMC chains. All the runs were performed in the cluster of the Institute of Theoretical Physics (IFT) in Madrid. This research is cofinanced by Greece and the European Union (European Social Fund—ESF) through the Operational Programme "Human Resources Development, Education and Lifelong Learning" in the context of the project "Strengthening Human Resources Research Potential via Doctorate Research—2nd Cycle" (MIS-5000432), implemented by the State Scholarships Foundation (IKY).

[1] P. A. R. Ade *et al.* (Planck Collaboration), Planck 2015 results. XIII. Cosmological parameters, Astron. Astrophys. **594**, A13 (2016).
[2] N. Aghanim *et al.* (Planck Collaboration), Planck 2018 results. VI. Cosmological parameters, arXiv:1807.06209.
[3] A. G. Riess, S. Casertano, W. Yuan, L. M. Macri, and D. Scolnic, Large Magellanic cloud Cepheid standards provide a 1% foundation for the determination of the Hubble constant and stronger evidence for physics beyond ΛCDM, Astrophys. J. **876**, 85 (2019).
[4] A. G. Riess, The expansion of the Universe is faster than expected, Nat. Rev. Phys. **2**, 10 (2019).
[5] W. D'Arcy Kenworthy, D. Scolnic, and A. Riess, The local perspective on the Hubble tension: Local structure does not impact measurement of the Hubble constant, Astrophys. J. **875**, 145 (2019).
[6] K. C. Wong *et al.*, H0LiCOW XIII. A 2.4% measurement of H_0 from lensed quasars: 5.3σ tension between early and late-Universe probes, arXiv:1907.04869.
[7] L. Verde, T. Treu, and A. G. Riess, Tensions between the early and the late Universe, Nat. Astron. **3**, 891 (2019).
[8] S. Taubenberger, S. H. Suyu, E. Komatsu, I. Jee, S. Birrer, V. Bonvin, F. Courbin, C. E. Rusu, A. J. Shajib, and K. C. Wong, The Hubble constant determined through an inverse distance ladder including quasar time delays and type Ia supernovae, Astron. Astrophys. **628**, L7 (2019).
[9] E. Macaulay, I. K. Wehus, and H. K. Eriksen, Lower Growth Rate from Recent Redshift Space Distortion Measurements than Expected from Planck, Phys. Rev. Lett. **111**, 161301 (2013).
[10] A. Johnson, C. Blake, J. Dossett, J. Koda, D. Parkinson, and S. Joudaki, Searching for modified gravity: Scale and redshift dependent constraints from galaxy peculiar velocities, Mon. Not. R. Astron. Soc. **458**, 2725 (2016).
[11] S. Tsujikawa, Possibility of realizing weak gravity in redshift space distortion measurements, Phys. Rev. D **92**, 044029 (2015).
[12] J. Solà, Cosmological constant *vis-à-vis* dynamical vacuum: Bold challenging the ΛCDM, Int. J. Mod. Phys. A **A31**, 1630035 (2016).
[13] S. Nesseris, G. Pantazis, and L. Perivolaropoulos, Tension and constraints on modified gravity parametrizations of $G_{\rm eff}(z)$ from growth rate and Planck data, Phys. Rev. D **96**, 023542 (2017).
[14] L. Kazantzidis and L. Perivolaropoulos, Evolution of the $f\sigma_8$ tension with the Planck15/ΛCDM determination and implications for modified gravity theories, Phys. Rev. D **97**, 103503 (2018).
[15] H. Hildebrandt *et al.*, KiDS-450: Cosmological parameter constraints from tomographic weak gravitational lensing, Mon. Not. R. Astron. Soc. **465**, 1454 (2017).
[16] F. Köhlinger *et al.*, KiDS-450: The tomographic weak lensing power spectrum and constraints on cosmological parameters, Mon. Not. R. Astron. Soc. **471**, 4412 (2017).
[17] S. Joudaki *et al.*, KiDS-450+2dFLenS: Cosmological parameter constraints from weak gravitational lensing tomography and overlapping redshift-space galaxy clustering, Mon. Not. R. Astron. Soc. **474**, 4894 (2018).
[18] T. M. C. Abbott *et al.* (DES Collaboration), Dark energy survey year 1 results: Cosmological constraints from galaxy clustering and weak lensing, Phys. Rev. D **98**, 043526 (2018).
[19] T. M. C. Abbott *et al.* (DES Collaboration), Dark energy survey year 1 results: Constraints on extended cosmological models from galaxy clustering and weak lensing, Phys. Rev. D **99**, 123505 (2019).
[20] S. Basilakos and S. Nesseris, Conjoined constraints on modified gravity from the expansion history and cosmic growth, Phys. Rev. D **96**, 063517 (2017).
[21] L. Kazantzidis and L. Perivolaropoulos, Is gravity getting weaker at low z? Observational evidence and theoretical implications, arXiv:1907.03176.
[22] É. Aubourg *et al.*, Cosmological implications of baryon acoustic oscillation measurements, Phys. Rev. D **92**, 123516 (2015).
[23] S. Alam *et al.* (BOSS Collaboration), The clustering of galaxies in the completed SDSS-III baryon oscillation spectroscopic survey: Cosmological analysis of the DR12 galaxy sample, Mon. Not. R. Astron. Soc. **470**, 2617 (2017).
[24] E. Macaulay *et al.* (DES Collaboration), First cosmological results using type Ia supernovae from the dark energy survey: Measurement of the Hubble constant, Mon. Not. R. Astron. Soc. **486**, 2184 (2019).
[25] M. Rigault *et al.*, Confirmation of a star formation bias in type Ia supernova distances and its effect on measurement of the Hubble constant, Astrophys. J. **802**, 20 (2015).
[26] B. R. Zhang, M. J. Childress, T. M. Davis, N. V. Karpenka, C. Lidman, B. P. Schmidt, and M. Smith, A blinded determination of H_0 from low-redshift Type Ia supernovae, calibrated by Cepheid variables, Mon. Not. R. Astron. Soc. **471**, 2254 (2017).
[27] S. Dhawan, S. W. Jha, and B. Leibundgut, Measuring the Hubble constant with Type Ia supernovae as near-infrared standard candles, Astron. Astrophys. **609**, A72 (2018).
[28] D. Fernández Arenas, E. Terlevich, R. Terlevich, J. Melnick, R. Chávez, F. Bresolin, E. Telles, M. Plionis, and S. Basilakos, An independent determination of the local Hubble constant, Mon. Not. R. Astron. Soc. **474**, 1250 (2018).
[29] W. L. Freedman *et al.*, The Carnegie-Chicago Hubble Program. VIII. An independent determination of the Hubble constant based on the tip of the red giant branch, Astrophys. J. **882**, 34 (2019).
[30] W. L. Freedman, B. F. Madore, T. Hoyt, I. Sung Jang, R. Beaton, M. Gyoon Lee, A. Monson, J. Neeley, and J. Rich, Calibration of the tip of the red giant branch (TRGB), Astrophys. J. **891**, 57 (2020).
[31] J. Richard Gott III, M. S. Vogeley, S. Podariu, and B. Ratra, Median statistics, H_0, and the accelerating universe, Astrophys. J. **549**, 1 (2001).
[32] G. Chen and B. Ratra, Median statistics and the Hubble constant, Publ. Astron. Soc. Pac. **123**, 1127 (2011).
[33] Y. Chen, S. Kumar, and B. Ratra, Determining the Hubble constant from Hubble parameter measurements, Astrophys. J. **835**, 86 (2017).
[34] H. Yu, B. Ratra, and F.-Y. Wang, Hubble parameter and baryon acoustic oscillation measurement constraints on the Hubble constant, the deviation from the spatially flat

ΛCDM model, the deceleration-acceleration transition redshift, and spatial curvature, Astrophys. J. **856**, 3 (2018).
[35] J. Zhang, Most frequent value statistics and the Hubble constant, Publ. Astron. Soc. Pac. **130**, 084502 (2018).
[36] A. Domínguez, R. Wojtak, J. Finke, M. Ajello, K. Helgason, F. Prada, A. Desai, V. Paliya, L. Marcotulli, and D. Hartmann, A new measurement of the Hubble constant and matter content of the Universe using extragalactic background light γ-ray attenuation, Astrophys. J. **885**, 137 (2019).
[37] H. Zeng and D. Yan, Using the extragalactic gamma-ray background to constrain the Hubble constant and matter density of the Universe, Astrophys. J. **882**, 87 (2019).
[38] Y. Wang, L. Xu, and G.-B. Zhao, A measurement of the Hubble constant using galaxy redshift surveys, Astrophys. J. **849**, 84 (2017).
[39] W. Lin and M. Ishak, Cosmological discordances II: Hubble constant, Planck and large-scale-structure data sets, Phys. Rev. D **96**, 083532 (2017).
[40] T. M. C. Abbott *et al.* (DES Collaboration), Dark energy survey year 1 results: A precise H_0 estimate from DES Y1, BAO, and D/H Data, Mon. Not. R. Astron. Soc. **480**, 3879 (2018).
[41] B. S. Haridasu, V. V. Lukovi ć, M. Moresco, and N. Vittorio, An improved model-independent assessment of the late-time cosmic expansion, J. Cosmol. Astropart. Phys. 10 (2018) 015.
[42] C.-G. Park and B. Ratra, Measuring the Hubble constant and spatial curvature from supernova apparent magnitude, baryon acoustic oscillation, and Hubble parameter data, Astrophys. Space Sci. **364**, 134 (2019).
[43] X. Zhang and Q.-G. Huang, Constraints on H_0 from WMAP and BAO measurements, Commun. Theor. Phys. **71**, 826 (2019).
[44] J. Ryan, Y. Chen, and B. Ratra, Baryon acoustic oscillation, Hubble parameter, and angular size measurement constraints on the Hubble constant, dark energy dynamics, and spatial curvature, Mon. Not. R. Astron. Soc. **488**, 3844 (2019).
[45] A. Cuceu, J. Farr, P. Lemos, and A. Font-Ribera, Baryon acoustic oscillations and the Hubble constant: Past, present and future, J. Cosmol. Astropart. Phys. 10 (2019) 044.
[46] W. Lin and M. Ishak, Remarks on measures of inconsistency, arXiv:1909.10991.
[47] C. Garcia-Quintero, M. Ishak, L. Fox, and W. Lin, Cosmological discordances. III. More on measure properties, large-scale-structure constraints, the Hubble constant and Planck data, Phys. Rev. D **100**, 123538 (2019).
[48] S. Alexander and E. McDonough, Axion-dilaton destabilization and the Hubble tension, Phys. Lett. B **797**, 134830 (2019).
[49] V. Poulin, T. L. Smith, T. Karwal, and M. Kamionkowski, Early Dark Energy Can Resolve The Hubble Tension, Phys. Rev. Lett. **122**, 221301 (2019).
[50] T. Karwal and M. Kamionkowski, Dark energy at early times, the Hubble parameter, and the string axiverse, Phys. Rev. D **94**, 103523 (2016).
[51] P. Agrawal, F.-Y. Cyr-Racine, D. Pinner, and L. Randall, Rock 'n' roll solutions to the Hubble tension, arXiv:1904.01016.
[52] M.-X. Lin, G. Benevento, W. Hu, and M. Raveri, Acoustic dark energy: Potential conversion of the Hubble tension, Phys. Rev. D **100**, 063542 (2019).
[53] M. Braglia, W. T. Emond, F. Finelli, A. Emir Gumrukcuoglu, and K. Koyama, Unified framework for early dark energy from α-attractors, arXiv:2005.14053.
[54] T. L. Smith, V. Poulin, and M. A. Amin, Oscillating scalar fields and the Hubble tension: A resolution with novel signatures, Phys. Rev. D **101**, 063523 (2020).
[55] J. Luis Bernal, L. Verde, and A. G. Riess, The trouble with H_0, J. Cosmol. Astropart. Phys. 10 (2016) 019.
[56] J. Sakstein and M. Trodden, Early Dark Energy from Massive Neutrinos—A Natural Resolution of the Hubble Tension, Phys. Rev. Lett. **124**, 161301 (2020).
[57] S. Ghosh, R. Khatri, and T. S. Roy, Dark neutrino interactions phase out the Hubble tension, arXiv:1908.09843.
[58] E. Di Valentino, A. Melchiorri, O. Mena, and S. Vagnozzi, Interacting dark energy after the latest Planck, DES, and H_0 measurements: An excellent solution to the H_0 and cosmic shear tensions, arXiv:1908.04281.
[59] W. Yang, S. Pan, E. Di Valentino, R. C. Nunes, S. Vagnozzi, and D. F. Mota, Tale of stable interacting dark energy, observational signatures, and the H_0 tension, J. Cosmol. Astropart. Phys. 09 (2018) 019.
[60] E. Di Valentino, A. Melchiorri, O. Mena, and S. Vagnozzi, Nonminimal dark sector physics and cosmological tensions, Phys. Rev. D **101**, 063502 (2020).
[61] W. Yang, A. Mukherjee, E. Di Valentino, and S. Pan, Interacting dark energy with time varying equation of state and the H_0 tension, Phys. Rev. D **98**, 123527 (2018).
[62] A. Gómez-Valent, V. Pettorino, and L. Amendola, Update on coupled dark energy and the H_0 tension, arXiv:2004.00610.
[63] K. Vattis, S. M. Koushiappas, and A. Loeb, Dark matter decaying in the late Universe can relieve the H_0 tension, Phys. Rev. D **99**, 121302 (2019).
[64] H. Desmond, B. Jain, and J. Sakstein, Local resolution of the Hubble tension: The impact of screened fifth forces on the cosmic distance ladder, Phys. Rev. D **100**, 043537 (2019); Erratum, Phys. Rev. D **101**, 069904 (2020).
[65] H. Desmond and J. Sakstein, Screened fifth forces lower the TRGB-calibrated Hubble constant too, arXiv:2003.12876.
[66] L. Kazantzidis and L. Perivolaropoulos, Hints of a local matter underdensity or modified gravity in the low z Pantheon data, arXiv:2004.02155.
[67] M. Rossi, M. Ballardini, M. Braglia, F. Finelli, D. Paoletti, A. A. Starobinsky, and C. Umiltà, Cosmological constraints on post-Newtonian parameters in effectively massless scalar-tensor theories of gravity, Phys. Rev. D **100**, 103524 (2019).
[68] M. Ballardini, F. Finelli, C. Umiltà, and D. Paoletti, Cosmological constraints on induced gravity dark energy models, J. Cosmol. Astropart. Phys. 05 (2016) 067.
[69] M. Braglia, M. Ballardini, W. T. Emond, F. Finelli, A. Emir Gumrukcuoglu, K. Koyama, and D. Paoletti, A larger value for H_0 by an evolving gravitational constant, arXiv:2004.11161.

[70] M.-X. Lin, M. Raveri, and W. Hu, Phenomenology of modified gravity at recombination, Phys. Rev. D **99**, 043514 (2019).
[71] V. V. Lukovi ć, B. S. Haridasu, and N. Vittorio, Exploring the evidence for a large local void with supernovae Ia data, Mon. Not. R. Astron. Soc. **491**, 2075 (2020).
[72] W. Yang, S. Pan, E. Di Valentino, E. N. Saridakis, and S. Chakraborty, Observational constraints on one-parameter dynamical dark-energy parametrizations and the H_0 tension, Phys. Rev. D **99**, 043543 (2019).
[73] W. Yang, S. Pan, A. Paliathanasis, S. Ghosh, and Y. Wu, Observational constraints of a new unified dark fluid and the H_0 tension, Mon. Not. R. Astron. Soc. **490**, 2071 (2019).
[74] X. Li and A. Shafieloo, A simple phenomenological emergent dark energy model can resolve the Hubble tension, Astrophys. J. Lett. **883**, L3 (2019).
[75] G. D'Amico, Z. Huang, M. Mancarella, and F. Vernizzi, Weakening gravity on redshift-survey scales with kinetic matter mixing, J. Cosmol. Astropart. Phys. 02 (2017) 014.
[76] M. Gonzalez-Espinoza, G. Otalora, J. Saavedra, and N. Videla, Growth of matter overdensities in non-minimal torsion-matter coupling theories, Eur. Phys. J. C **78**, 799 (2018).
[77] J. Kennedy, L. Lombriser, and A. Taylor, Reconstructing Horndeski theories from phenomenological modified gravity and dark energy models on cosmological scales, Phys. Rev. D **98**, 044051 (2018).
[78] E. V. Linder, No slip gravity, J. Cosmol. Astropart. Phys. 03 (2018) 005.
[79] J. Solà, A. Gómez-Valent, and J. de Cruz Pérez, The H_0 tension in light of vacuum dynamics in the Universe, Phys. Lett. B **774**, 317 (2017).
[80] A. Gómez-Valent and J. Solà Peracaula, Density perturbations for running vacuum: A successful approach to structure formation and to the σ_8-tension, Mon. Not. R. Astron. Soc. **478**, 126 (2018).
[81] J. Ooba, B. Ratra, and N. Sugiyama, Planck 2015 constraints on the non-flat ΛCDM inflation model, Astrophys. J. **864**, 80 (2018).
[82] C.-G. Park and B. Ratra, Using the tilted flat-ΛCDM and the untilted non-flat ΛCDM inflation models to measure cosmological parameters from a compilation of observational data, Astrophys. J. **882**, 158 (2019).
[83] A. Pourtsidou and T. Tram, Reconciling CMB and structure growth measurements with dark energy interactions, Phys. Rev. D **94**, 043518 (2016).
[84] S. Joudaki *et al.*, KiDS-450: Testing extensions to the standard cosmological model, Mon. Not. R. Astron. Soc. **471**, 1259 (2017).
[85] F. Melia, The linear growth of structure in the $R_h = ct$ universe, Mon. Not. R. Astron. Soc. **464**, 1966 (2017).
[86] S. Camera, M. Martinelli, and D. Bertacca, Does quartessence ease cosmic tensions?, Phys. Dark Universe **23**, 100247 (2019).
[87] A. Gomez-Valent and J. Sola, Relaxing the σ_8-tension through running vacuum in the Universe, Europhys. Lett. **120**, 39001 (2017).
[88] J. Ooba, B. Ratra, and N. Sugiyama, Planck 2015 constraints on spatially-flat dynamical dark energy models, Astrophys. Space Sci. **364**, 176 (2019).
[89] B. J. Barros, L. Amendola, T. Barreiro, and N. J. Nunes, Coupled quintessence with a ΛCDM background: Removing the σ_8 tension, J. Cosmol. Astropart. Phys. 01 (2019) 007.
[90] G. Lambiase, S. Mohanty, A. Narang, and P. Parashari, Testing dark energy models in the light of σ_8 tension, Eur. Phys. J. C **79**, 141 (2019).
[91] S. Vagnozzi, New physics in light of the H_0 tension: An alternative view, arXiv:1907.07569.
[92] E. Di Valentino, A. Melchiorri, and J. Silk, Reconciling Planck with the local value of H_0 in extended parameter space, Phys. Lett. B **761**, 242 (2016).
[93] Q.-G. Huang and K. Wang, How the dark energy can reconcile Planck with local determination of the Hubble constant, Eur. Phys. J. C **76**, 506 (2016).
[94] E. Di Valentino, A. Melchiorri, E. V. Linder, and J. Silk, Constraining dark energy dynamics in extended parameter space, Phys. Rev. D **96**, 023523 (2017).
[95] X. Li and A. Shafieloo, Generalised emergent dark energy model: Confronting Λ and PEDE, arXiv:2001.05103.
[96] M. Rezaei, T. Naderi, M. Malekjani, and A. Mehrabi, A Bayesian comparison between ΛCDM and phenomenologically emergent dark energy models, Eur. Phys. J. C **80**, 374 (2020).
[97] G. Efstathiou and J. R. Bond, Cosmic confusion: Degeneracies among cosmological parameters derived from measurements of microwave background anisotropies, Mon. Not. R. Astron. Soc. **304**, 75 (1999).
[98] O. Elgaroy and T. Multamaki, On using the CMB shift parameter in tests of models of dark energy, Astron. Astrophys. **471**, 65 (2007).
[99] W. Hu and N. Sugiyama, Small scale cosmological perturbations: An analytic approach, Astrophys. J. **471**, 542 (1996).
[100] Y. Wang and P. Mukherjee, Robust dark energy constraints from supernovae, galaxy clustering, and three-year Wilkinson Microwave Anisotropy Probe observations, Astrophys. J. **650**, 1 (2006).
[101] M. Chevallier and D. Polarski, Accelerating universes with scaling dark matter, Int. J. Mod. Phys. D **10**, 213 (2001).
[102] E. V. Linder, Exploring the Expansion History of the Universe, Phys. Rev. Lett. **90**, 091301 (2003).
[103] L. Kazantzidis, L. Perivolaropoulos, and F. Skara, Constraining power of cosmological observables: Blind redshift spots and optimal ranges, Phys. Rev. D **99**, 063537 (2019).
[104] G. Benevento, W. Hu, and M. Raveri, Can late dark energy transitions raise the Hubble constant?, Phys. Rev. D **101**, 103517 (2020).
[105] G.-B. Zhao, L. Pogosian, A. Silvestri, and J. Zylberberg, Searching for modified growth patterns with tomographic surveys, Phys. Rev. D **79**, 083513 (2009).
[106] A. Hojjati, L. Pogosian, and G.-B. Zhao, Testing gravity with CAMB and CosmoMC, J. Cosmol. Astropart. Phys. 08 (2011) 005.
[107] A. Zucca, L. Pogosian, A. Silvestri, and G.-B. Zhao, MGCAMB with massive neutrinos and dynamical dark energy, J. Cosmol. Astropart. Phys. 05 (2019) 001.

[108] B. Sagredo, S. Nesseris, and D. Sapone, Internal robustness of growth rate data, Phys. Rev. D **98**, 083543 (2018).
[109] F. Skara and L. Perivolaropoulos, Tension of the E_G statistic and redshift space distortion data with the Planck-ΛCDM model and implications for weakening gravity, Phys. Rev. D **101**, 063521 (2020).
[110] D. M. Scolnic *et al.*, The complete light-curve sample of spectroscopically confirmed SNe Ia from Pan-STARRS1 and cosmological constraints from the combined Pantheon sample, Astrophys. J. **859**, 101 (2018).
[111] F. Beutler, C. Blake, M. Colless, D. Heath Jones, L. Staveley-Smith, L. Campbell, Q. Parker, W. Saunders, and F. Watson, The 6dF Galaxy survey: Baryon acoustic oscillations and the local Hubble constant, Mon. Not. R. Astron. Soc. **416**, 3017 (2011).
[112] A. J. Ross, L. Samushia, C. Howlett, W. J. Percival, A. Burden, and M. Manera, The clustering of the SDSS DR7 main Galaxy sample—I. A 4 per cent distance measure at $z = 0.15$, Mon. Not. R. Astron. Soc. **449**, 835 (2015).
[113] N. Arendse *et al.*, Cosmic dissonance: New physics or systematics behind a short sound horizon?, arXiv: 1909.07986.
[114] L. Perivolaropoulos, Crossing the phantom divide barrier with scalar tensor theories, J. Cosmol. Astropart. Phys. 10 (2005) 001.
[115] P. J. E. Peebles and B. Ratra, Cosmology with a time variable cosmological constant, Astrophys. J. Lett. **325**, L17 (1988).
[116] B. Ratra and P. J. E. Peebles, Cosmological consequences of a rolling homogeneous scalar field, Phys. Rev. D **37**, 3406 (1988).
[117] I. Zlatev, L.-M. Wang, and P. J. Steinhardt, Quintessence, Cosmic Coincidence, and the Cosmological Constant, Phys. Rev. Lett. **82**, 896 (1999).
[118] T. Chiba, T. Okabe, and M. Yamaguchi, Kinetically driven quintessence, Phys. Rev. D **62**, 023511 (2000).
[119] D. Polarski, A. A. Starobinsky, and H. Giacomini, When is the growth index constant?, J. Cosmol. Astropart. Phys. 12 (2016) 037.
[120] R. Gannouji, L. Kazantzidis, L. Perivolaropoulos, and D. Polarski, Consistency of modified gravity with a decreasing $G_{\rm eff}(z)$ in a ΛCDM background, Phys. Rev. D **98**, 104044 (2018).
[121] https://github.com/GeorgeAlestas/H0_Tension_Data.